HAL open science

An improved biologically plausible trajectory generator

Thierry Viéville

▶ To cite this version:

Thierry Viéville. An improved biologically plausible trajectory generator. [Research Report] RR-4539, INRIA. 2002. inria-00072049

HAL Id: inria-00072049

https://inria.hal.science/inria-00072049v1

Submitted on 23 May 2006

HAL is a multi-disciplinary open access archive for the deposit and dissemination of scientific research documents, whether they are published or not. The documents may come from teaching and research institutions in France or abroad, or from public or private research centers.

L'archive ouverte pluridisciplinaire **HAL**, est destinée au dépôt et à la diffusion de documents scientifiques de niveau recherche, publiés ou non, émanant des établissements d'enseignement et de recherche français ou étrangers, des laboratoires publics ou privés.

INSTITUT NATIONAL DE RECHERCHE EN INFORMATIQUE ET EN AUTOMATIQUE

An improved biologically plausible trajectory generator

T. Viéville

N° 4539 – version 2

version initiale Septembre 2002 – version révisée Février 2006

Thème BIO

Rapport de recherche

ISSN 0249-6399

An improved biologically plausible trajectory generator

T. Viéville

Thème BIO — Systèmes biologiques
Projet Odyssee

Rapport de recherche n° 4539 – version 2*— version initiale Septembre 2002 — version révisée Février 2006 34 pages

Abstract:

Considering the biological or artificial trajectory generation problem, we propose a biologically plausible model of the link between the (i) local "where-to-go-next" local mechanism in a locus map and the (ii) global trajectory generation problem. This explains how the well known hippocampal related areas containing locus-maps with local mechanisms are also very likely able to solve the global problem, providing the neural map activity is related to harmonic potentials.

Such representation assume that obstacles to avoid (or constraints not to violate) correspond to maxima of a so-called potential, while the goal corresponds to its minimum. The corresponding algorithm thus behaves as if one throws a sheet onto this state space, this hyper-surface relief being elevated on obstacles, with a hole at the goal location. Finding a trajectory thus reduces to "roll down" along this relief, in the direction of the potential gradient.

The originality of the present work is to build an harmonic potential (thus without local minimum) from a sparse adpative combination of elementary locus, as inspired by the biological modelization of the hippocampal structures.

This leads to an internal representation of the problem as a non-topographical map, incrementally built during the system exploration. As such, it provides a key element for a biologically plausible model of the related hippocampus mechanisms in coherence with usual biological assumptions about such behavior.

Version 2 of RR 4539 with more experimentation, some extensions of the method and a formal demonstration of the adaptive algorithm convergence.

Key-words: Trajectory generation, Harmonic potential, Biological model

* This version has more experimentation, some extensions of the method and a formal demonstration of the adaptive algorithm convergence.

Un générateur de trajectoire biologiquement plausible amélioré

Résumé :

Considérant le contrôle biologique ou artificiel de la génération d'une trajectoire, nous présentons ici un modèle biologiquement plausible basé sur une méthode dite de potentiel harmonique.

Les méthodes à base de potentiel supposent que les obstacles à éviter (ou les contraintes à ne pas enfreindre) correspondent à des maxima de ce potentiel tandis que le but à atteindre est un unique minimum. L'algorithme se comporte comme si l'on jetait un drap sur cet espace, formant des bosses aux obstacles et un creux vers le but; trouver une trajectoire revient alors à se «laisser glisser» le long de ce drap vers le point de hauteur minimale. Ces méthodes permettent de passer du «local au global» en ce sens qu'une minimisation locale du potentiel permet finalement de trouver une trajectoire globale, choisir un itinéraire, etc..

L'originalité de la présente méthode est de construire un potentiel harmonique (donc sans minimum local) comme une combinaison linéaire finie de fonctions harmoniques élémentaires. L'ensemble de ces éléments forme un échantillonnage de la frontière du domaine admissible, bordé par les obstacles ou contraintes. Cela conduit à une représentation interne du problème sous la forme d'une carte non-topographique construite au fur et à mesure des évolutions du système et reliée de manière non-linéaire à la géométrie du problème réel. En tant que tel, cela fournit un modèle quantitatif biologiquement plausible du fonctionnement de l'hippocampe et des cartes cognitives qui y sont représentées, cohérent avec les hypothèses biologiques usuelles.

Version 2 du RR 4539 avec plus d'expérimentation, quelques extensions de la méthode et une démonstration formelle de la convergence de l'algorithme adaptatif.

Mots-clés : Génération de trajectoire, Potentiel harmonique, Modèle biologique

Contents

1 Introduction **3**

2 Harmonic locus maps. **8**

3 Experimenting trajectory generation **22**

4 Conclusion **27**

A Using an harmonic potential with unbounded values **32**

1 Introduction

The "trajectory generation" problem.

We consider here the biological or artificial generation of a trajectory (please refer to e.g. [19] for an introduction) and would like to propose a biologically plausible model of such a mechanism.

Finding a "trajectory" from an initial state, to a final state, is a very general problem: if the state is a 3D or 2D position in our Euclidean space or on a geographical map, it indeed means finding its way in a cluttered space for instance, avoiding touching the road border, choosing between two paths, and so on. The boundary of an obstacle may be defined by an equation, say $c(\mathbf{x}) = 0$, with the constraint $c(\mathbf{x}) > 0$ for "admissible" points $\mathbf{x}$ outside the obstacle. The goal may similarly be defined by an inequality to be satisfied.

But trajectory generation also means something more general. For instance, let us now consider the position $\mathbf{x}$ and velocity $\dot{\mathbf{x}}$ of the device. Constraints of the form $c(\mathbf{x}, \dot{\mathbf{x}}) > 0$ may define how to avoid skid, or bound the instantaneous energy consumption. More generally, constraints which correspond to physical laws not to violate can be written in such a form. For instance, when maneuvering to park a car (which can be defined as small sequence of locations to attain) we cannot move "laterally" but have to follow a realistic trajectory: this can also be specified as a constraint [7]. Similarly, during robotic surgery (see e.g [10] for an example related to cardiology) a device with a large number of degrees of freedom, has to generate a highly constrained "trajectory" from the initial configuration toward the surgery location inside the body. A step ahead, a planning task such as the realization of a "gesture" may be specified as an "abstract" trajectory generation problem, defined by some quantitative parameters (a state vector) with an initial state and a goal to attain while verifying constraints.

Such a problem has to be solved:
(i) "during action" since the trajectory generation is also an exploration of the state space, thus with the potential discovery of another constraints (at the difference of a predefined "motor-program" which realization is less in relation with exploration),
(ii) "at a global level" since the goal to attain is a remote part of the state space while local

mechanisms are not sufficient to solve such a problem (at a difference of a "reflex" or a local "feedback" loop)
(iii) considering state spaces with "large" dimensions because the dimension to consider is the number of degree of freedoms of the problem.

As a computational problem [19, 1, 9] it is usually very hard to solve because this *large dimensional global problem* is almost always non-linear. The object to find is a "curve" i.e. an object which an infinite dimension. When approximated by a set of segments, finding this curve easily leads to a combinatorial explosion.

About biological trajectory generators.

Contrary to this apparent complexity, small mammalian very easily solve trajectory generation problems, including with combinatorial complexity (e.g. rats in labyrinths as discussed in [28, 2]): it is obvious that the survival of a biological system, pray or predator, is directly related to its capacity to correctly execute a trajectory in a known or unknown environment: find its way to a water source, follow an olfactory track avoiding negative smells or odors, etc..

The hippocampus is 1st the sub-cortical structure which has been shown [21] to be directly involved in such mechanisms[1]. As reviewed in, e.g. [2], the fact hippocampal lesions drastically impair the ability of rodents to navigate has led to the assumption that hippocampus plays an important role in navigation by providing a cognitive map stored by potential synaptic weights representing both spatial and temporal correlations. According to [2], the stored information is related to locations and position shifts coded by place cell activity that arise from synaptic potentiation.

The hippocampus and related areas are indeed not the only one structure with "locus" or place cells or involved in planning. However, we restrict our discussion to these structures because we want to discuss rather precise properties of such maps, and relate them to the proposed model, as presented now and discussed in the sequel.

More precisely, we consider the architecture of the hippocampal structures, mainly the entorhinal cortex → dentral gyrus → CA3/CA1 (Corpus Ammonis is another name of the hippocampus) in the hippocampus → prefrontal/striatum areas (see for instance [12] for an extended discussion about the spatial aspects of the hippocampus functionality and [20] for a discussion about other perceptual and motor tasks of the hippocampus), as illustrated in Fig. 1.

[1] *About locus cells.* The key experimental fact is the discovery of "locus cells" [21] in the hippocampus. Summarizing, such cells have the property to becomes active when the animal is at a given location in the environment and:
(i) corresponds to a space location which is a order of magnitude larger than the animal size,
(ii) continue to fire even if the environment tokens are removed or if the animal is in the dark,
(iii) are used for different locations in different environments,
(iv) have various shapes without any direct link with the environment metric,
(v) have, for a sub-set of such cells, an activity not only related to the location but also to the local trajectory direction,
(vi) such cells starts firing as soon as the animal entered the corresponding environment.

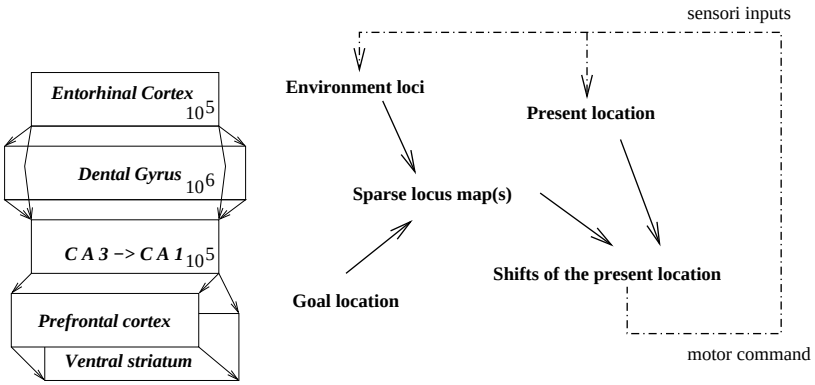

Figure 1: Architecture of the main stream and state variables of the related hippocampal structures, see text for details.

In this architecture (see e.g. [30] for a general discussion and e.g. [25] for a recent review) information about loci is input from the entorhinal cortex which integrates several source of information, including spatial ones. The expansion layer role is likely to dispatch this information, "allocating" locus cells (see e.g. [15] for a detailed discussion). The compression layer role is likely to combine and sum-up the locus cell combinations building the location shift output in the CA1 structure towards motor areas via the ventral striatum. The subject location is also coded in these parts of the hippocampal formation.

In recent biological models, the prefrontal structure is though responsible for encoding goal location, although there are also evidences that hippocampal locus cells related to goal locations increase their activity. This may be due to interactions between both maps. The key point here is that more than one map likely interact in the sensori-motor loop involved in trajectory generation. A computational model must take such locus-map combination into account.

Another crucial aspect is the fact that loci are not organized topographically, whereas for a given spatial-area loci are "recruited" without any spatial sortering when required. For a given spatial-area, about 40% of the cells are recruited. This very important property must be present in a computational model. The location is related to the spatial-area frame of reference, due to both external sensory cues (mainly visual but not only) and idiothetic (self-motion related) interacting with each-other. The subject location is "calibrated" with respect to this spatial map.

During the transition between two spatial-areas, the set of loci are re-activated in the locus map, eventually re-using a previously registered locus map and eventually updating it with new incoming information. Such locus map is thus remanent with respect to the sensory input (stored representation of the surroundings). During navigation between unconnected portions of space, there is a switch between locus maps. The way a computational model

can implement such a property is a also a key issue. Here, locus cells are actively involved in relation not to object identity but location.

Another aspect, appearing in previous references, is that neural sites related to loci corresponding to "obstacles" (i.e. at the border of the spatial-area) have elongated shapes. Such an anisotropic shape might be related to the fact loci at the border of the spatial-area reflects the border topology, in the sense that what is on the other side of the border is likely not represented on the map. On the contrary loci corresponding to intermediate goals have an isotropic shape.

Locus cells related to inside the spatial-area are less present but isotropic: the role of such loci may be related to intermediate obstacles but also in relation with intermediate goal(s).

Comparing goal oriented tasks related to navigational behaviors with respect to wandering tasks without a precise goal to attain, there are only subtle differences in CA1 firing characteristics (mainly a marginal increase of the firing rate in the 1st case). This result is compatible with the fact that the goal location is encoded elsewhere (e.g. in the prefrontal cortex) and shows that both kind of behaviors likely use the same mechanisms.

Modern ideas about neural bases of navigation seems to defeat some of the usual concepts about related cognitive maps[2] and it is not clear if apparently different behaviors (goal oriented versus wandering exploration, spatial versus beacon (or token based) navigation, metric versus topological navigation) are not different facets of the same mechanism:
- beacon navigation can be viewed as a goal related navigation with several intermediate sub-goals;
- exploration can be viewed as a limit case of goal directed navigation with a weak or evanescent goal;
- metric navigation may be a consequence of the generation of an optimal path towards a goal but using any non-metric representation, etc..

[2] *About cognitive maps.* A taxonomy of the different strategies related to such cognitive maps is detailed in [30] from the simple repulsion/attraction mechanisms (e.g. a bee orientation with respect to the sun) to sophisticated metric map navigation (e.g. a human in a car). Very briefly, according to the authors, such behavior requires the autonomous locomotion of the agent and the notion of attraction/repulsion and may be structured in terms of :

+ *"guided navigation"*, where the subject attempts to memorize the sequence of perceptions received during the previous navigation and locally modifies its behavior to reproduce this sequence,

+ *"associative navigation"*, where the subject memorizes for each "location" a "new direction" and navigate by passing from one location to another using the "direction field",

+ *"topological navigation"*, where the subject has memorized a graph of the locations (nodes of the graph) and of the paths (vertices of the graph) from one location to another, while it navigates by identifying the sequence of locations from its location to the goal,

+ *"metric navigation"*, where the subject has now a metric, i.e. topographic, map and identify not only the sequence of locations but also consider the length of the trajectory, eventually *considering new paths not explored previously* and also introducing *shortcuts or roundabout* (see [22] for a precise discussion on this subject).

In this taxonomy, the idea of "cognitive maps" as proposed by [29] is introduced, which defines an internal representation of the environment used by the animal to find its way.

Emerging concepts [17] tend to integrate in a common framework these apparently different behaviors (contrary to very complex mechanisms such as those proposed in e.g. [26] in order to explain the different aspects of these behaviors).

Following this track, a computational model must not only describe how to learn the spatial property of the environment, but also address the global problem of trajectory generation because (see e.g. for a demonstrative example [24]) internal representations are always built in deep relation with their related sensori-motor task: here the spatial map is built in relation with the navigation task (see, for example the discussion in, [27], where it is also shown that heading direction is responsible for the implementation of angular path integration).

At this point it appears that all hippocampal related mechanisms, although much more complex than what is briefly reviewed here, are only related to the local "where-to-go-next" aspect of the trajectory generation. And the question to relate this local mechanism, as schematized in the right part of Fig. 2 to the global trajectory generation problem in a sensory-motor loop remains an issue.

This is the aspect we want to address here, showing that with a suitable locus cell representation the local "where-to-go-next" local mechanism directly relates to the global trajectory generation problem and provides a solution to it, fully compatible with the aspects reviewed here. Let us introduce this idea now.

Using potential to generate trajectories

In computer science, one track (see for instance [1, 9] for works at the origin of this one) to solve the navigation problem is to represent the trajectory generation problem using a so-called *potential*. Such methods assume that obstacles to avoid (or constraints not to violate) correspond to maxima of the potential, while the goal corresponds to a unique minimum. The corresponding algorithm thus behaves as if one throws a sheet onto this state space, this hyper-surface relief being elevated on obstacles, with a hole on the goal, so that finding a trajectory reduces to "roll down" in the direction of the potential gradient.

However, when building such a potential the main problem is the occurrence of local minima (see for instance [36] for a simple closed-form illustrating this statement). For instance, a concave obstacle may "hide" the goal and generate a local minimum, where the trajectory is trapped. Such a situation very likely occurs [19]. Techniques to manage this caveat exist: for instance in [1], points where the gradient is an eigen-vector of the Hessian of the potential allows to define a road-map onto which trajectories may be generated avoiding local minimum. However, such mechanisms are far from being trivial to implement. Furthermore, they have no link with biological mechanisms.

An elegant solution has been introduced by Connolly and Grupen [9, 7, 8] considering *harmonic functions as potentials*: it is well known that such a function has no minimum except on the domain boundaries (see e.g. [13] or appendix A for a short review on harmonic functions properties). This approach also allows to introduce non-holonomic constraints [7] (i.e. solve the trajectory generation problem even if the underlying mechanical system to control is singular in the sense that local control loops fails driving it). The Connolly and

Grupen approach also allows to relate such a potential to an obstacle collision probability [8], generating a trajectory with some statistical optimality with respect to obstacle avoidance. Recently (e.g. [6]), this group has a developed biological model of behavior using this approach as discussed in the sequel.

In their implementation, the authors calculate the potential on a regular mesh, sampling the state space. The drawback of such an implementation is indeed the large memory consumption and the huge computation time. For instance, for a problem with 6 degrees of freedom (e.g. a robotic arm) with parameter precision of, says, 0.1 % this yields to a regular mesh of .. 10^{18} units. This is thus intractable. Indeed, several heuristics (e.g. hierarchical/adaptive [14]) may reduce this complexity, but not its order of magnitude, while any sampling complexity has intrinsically an exponential growth with the space dimension (e.g. [3] for a recent discussion regarding triangulation of high-dimensional space), whatever the space triangulation or mesh method is. As a consequence, this method has been, in practice, not really used for dimensions higher than $n = 2$ or $n = 3$ (see for instance [1, 7]).

Furthermore, the numerical convergence may be very slow, because the influence of the goal (which introduces a slope in the potential relief in order to attract the trajectory) must be propagated though the whole state space by the numerical scheme used to compute the harmonic potential (see e.g. [4] for details) to be taken into account in remote locations.

In order to avoid the previous bad situation, the present work aims at building an harmonic potential (thus without local minimum) as a sparse finite linear combination of elementary harmonic functions. It appears that such a construction is in direct link with what is presently understood regarding hippocampal related structures.

In the following section we formally review the problem and introduce a sparse adaptive form of parametrized unbounded harmonic potential, called an *adelician*. We show that this family of potential solves the present problem.

We also discuss how this may lead to an internal representation of the problem as a non-topographic map in relation with the hippocampus mechanisms and the related cognitive maps.

In the next section we describe how we can implement such a mechanism. Two "toy" experiments are reported, which results allow to analyze the qualitative properties of this mechanism.

2 Harmonic locus maps.

Problem formalization

Let us consider:

(a) a system, defined by a *state vector* $\mathbf{x} \in \mathcal{R}^n$, $n \geq 2$

(b) an *initial state*, written $\mathbf{x}_0 \in \mathcal{R}^n$,

(c) r *constraints* defined by scalar inequalities $c_i(\mathbf{x}) > 0, i \in \{1..r\}$,

(d) a *goal* defined by an constraint of the form $c_0(\mathbf{x}) \leq 0$,

as illustrated in Fig. 2.

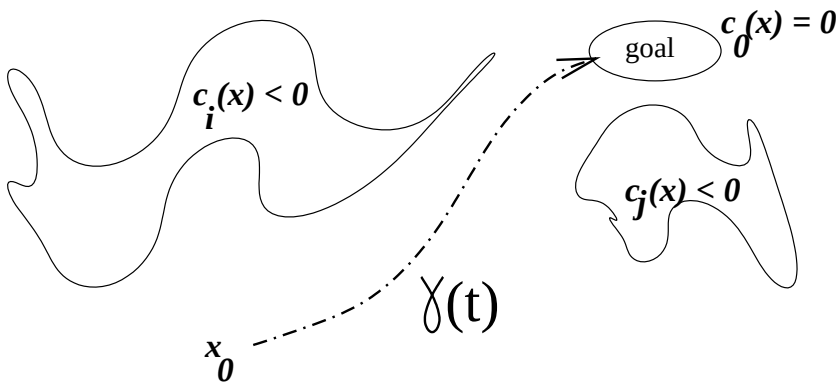

Figure 2: Schematic view of the trajectory generation problem.

The problem is thus defined using implicit equations $c_i : \mathcal{R}^n \to \mathcal{R}$ (assumed to be at least twice differentiable, or considering distributions).

If the goal is simply to reach a final state $\mathbf{x}_\infty \in \mathcal{R}^n$ (i.e. a punctual goal), the related implicit equation is, say, $c_0(\mathbf{x}) = ||\mathbf{x} - \mathbf{x}_\infty||$.

This defines a domain:

$$\mathcal{U} = \{\mathbf{x}, \forall i \in \{0..r\}, c_i(\mathbf{x}) > 0\}$$

assumed to be *connected* with $\mathbf{x}_0 \in \mathcal{U}$ and which frontier is:

$$\partial\mathcal{U} = \{\mathbf{x}, \exists i \in \{0..r\}, c_i(\mathbf{x}) = 0\} = \cup_{i=0}^{r} \partial\mathcal{U}_i$$

where $\partial\mathcal{U}_i = \{\mathbf{x}, c_i(\mathbf{x}) = 0\}$ is the frontier of the ith constraint/obstacle (if $i > 0$) or the frontier of the goal (if $i = 0$).

We write $\bar{\mathcal{U}} = \mathcal{U} \cup \partial\mathcal{U}$ the state space of this problem.

Concretely, $\mathbf{x}$ contains physical parameters. They are thus bounded quantities and we can assume that $\mathcal{U}$ is bounded, so that $\bar{\mathcal{U}}$ is *compact*.

Here we look for a trajectory $\gamma : \mathcal{R}^+ \to \mathcal{R}^n$ such that:

- it starts at the initial point $\gamma(0) = \mathbf{x}_0$,
- verifies the problem constraints $\forall t \in \mathcal{R}^+, \gamma(t) \in \mathcal{U}$,
- reaches (at least asymptotically) the goal $\lim_{t\to\infty} c_0(\gamma(t)) = 0$,

this trajectory being continuous and at least twice differentiable.

The differentiability condition allows to correctly control the trajectory execution by a physical device. In fact, the solution proposed in the sequel yields infinite differentiability.

Introducing harmonic potential

In order to solve the present problem we introduce a potential $V : \mathcal{U} \rightarrow \mathcal{R}$ which minimization allows to generate the expected trajectory $\gamma()$:

(i) starting for the initial point
(ii) looking for a smaller value of $V()$ at each step
(iii) stopping when the minimum of $V()$ is reached

More precisely, we consider trajectories $\gamma(t)$ such that:

$$\gamma'(t) = -\nabla V(\gamma(t)) \tag{1}$$

which is a standard 1st order minimization scheme, since:

$$V'(\gamma(t)) = \nabla V(\gamma(t))^T \gamma'(t) = -||\nabla V(\gamma(t))||^2 < 0$$

As such, this potential not only allows to find a trajectory from a given $\mathbf{x}_0$ to the goal, but from any $\mathbf{x}_0 \in \mathcal{U}$ to the goal: we thus have embedded the present problem in a more general one, in order to be able to solve it.

In order this paradigm to be valid, we introduce the following constraints:

$\mathcal{C}_0$ The goal corresponds to minima of the potential. Here we choose:

$$\lim_{\mathbf{x} \rightarrow \partial \mathcal{U}_0} V(\mathbf{x}) = -\infty \tag{2}$$

$\mathcal{C}_i$ Obstacles are maxima of the potential. Here we choose:

$$\forall i, \lim_{\mathbf{x} \rightarrow \partial \mathcal{U}_i} V(\mathbf{x}) = +\infty \tag{3}$$

$\mathcal{C}_c$ There is no local minimum (or flat regions) of the potential:

$$\forall \mathbf{x} \in \mathcal{U}, ||\nabla V(\mathbf{x})|| > 0$$

Here we choose an *harmonic potential*:

$$\forall \mathbf{x} \in \mathcal{U}, \Delta V(\mathbf{x}) = 0 \tag{4}$$

which, as detailed in appendix A, allows to verify $\mathcal{C}_c$.

Choosing unbounded values on the domain border may look like a strange choice but leads to a surprisingly simple *closed-form* solution developed now. At the implementation level, bounded potentials are going to be easily derived from this closed-form solution. The technical consequences of accepting infinite values on the domain boundaries of an harmonic potential are discussed in appendix A. This representation is motivated by the fact that finding an explicit solution for a bounded harmonic potential seems an intractable problem [13] while any numerical solutions are limited by the curse of dimensionality [1, 7] in this case.

Choosing an harmonic potential is far from being the only one solution (e.g. defining a convex potential is a less constrained alternative) but has a very interesting optimal property:

it *minimizes the average value of the kinetic energy* for all trajectories defined from this potential, since the so-called Dirichlet principle (see again e.g. [13] and $\mathcal{P}_5$ in appendix A for a technical remark regarding unbounded potential) is verified and the quantity $\int_{\mathcal{V}} ||\nabla V(\mathbf{x})||^2$ is minimal on any subset $\mathcal{V} \subset\subset \mathcal{U}$ in direct relation with the trajectory kinetic energy from (1) since proportional to the square of the velocity. As developed in [8] this also corresponds to a *minimum of the obstacle collision probability*. It is thus the "cheaper" and "safer" choice, better than e.g. minimal length trajectory[3].

Defining an *adelician*

When solving $\mathcal{C}_0$, $\mathcal{C}_i$ and $\mathcal{C}_c$ we define, by analogy with the Green formula (property $\mathcal{P}_6$ in appendix A), for any set of bounded measures on the domain border $\mu_i : \partial\mathcal{U}_i \to \mathcal{R}^+, i \in \{0..r\}$, the related *adelician* of the present problem:

$$\mathcal{A}(\mathbf{x}) = \sum_{i=1}^{r} \mathcal{A}_i(\mathbf{x}) - \mathcal{A}_0(\mathbf{x}) \text{ with } \mathcal{A}_i(\mathbf{x}) = \int_{\partial\mathcal{U}_i} \Phi(\mathbf{x}-\mathbf{y})\, \mu_i(\mathbf{y})\, d\mathbf{y} \tag{5}$$

where, for $n > 2$, $\Phi(\mathbf{x}) = \frac{\lambda}{||\mathbf{x}||^{n-2}}$, for some λ, is the fundamental radial symmetric harmonic function, as defined in (14).

Such a potential:

- is well-defined in $\mathcal{U}$, since the integrals used to define $\mathcal{A}_i(\mathbf{x})$ are summable,
- verifies $\Delta\mathcal{A}(\mathbf{x}) = 0$ in $\mathcal{U}$ as a linear combination of harmonic functions,
- verifies the boundaries conditions (2) and (3).

Considering (2):

$$\begin{aligned}
&\lim_{\mathbf{x}\to\mathbf{x}_0\in\partial\mathcal{U}_0} \mathcal{A}(\mathbf{x}) \\
&= \lim_{\mathbf{x}\to\mathbf{x}_0\in\partial\mathcal{U}_0} \mu_0(\mathbf{x}_0)\, \Phi(\mathbf{x}-\mathbf{x}_0) && \text{since all quantities except } \Phi(\mathbf{x}-\mathbf{x}_0) \text{ remain bounded} \\
&= +\infty && \text{from the definition of } \Phi(),\ \mu_0() \text{ being bounded}
\end{aligned}$$

and a similar result occurs for (3)

These adelicians thus define a family of solutions of the problem.

For example, a canonical example of solution is defined when choosing $\mu_i(\mathbf{x}) = 1$ on the domain border, i.e.:

$$\mu_i(\mathbf{x}) = Y(-c_i(\mathbf{x})) \tag{6}$$

[3] *About minimal length trajectory.* Intuitively (see [36] for a more formal discussion), a minimal length or minimal energy solution corresponds to rectilinear segments (the shortest way from one point to another) unless encountering an obstacle and then moving in a small neighborhood of the obstacle, until yet another rectilinear trajectory segment. Such solutions are not very attractive because as soon as a small numerical uncertainty occurs the constraint related to the obstacle is easily violated.
On the contrary, potential minimization (with obstacle repulsion) refrains the trajectory to get close to obstacles we also obtain a kind of "risk" minimization.
Here the key point is that this risk minimization is compatible with energy minimization.

where $Y(u) =$ if $u > 0$ then 1 elif $u < 0$ then 0 is the Heaviside distribution.

In fact, **for $n > 2$ adelicians define the family of solutions of the problem stated in $\mathcal{C}_0$, $\mathcal{C}_i$ and $\mathcal{C}_c$.**

Let us consider an harmonic potential $V(\mathbf{x})$ such that

$$\lim_{\mathbf{x}\to\mathbf{x}_\bullet\in\partial\mathcal{U}} V(\mathbf{x}) = +\infty$$

and consider polar coordinates around $\mathbf{x}_\bullet$ i.e. write $\mathbf{x} = \mathbf{x}_\bullet + \rho\,\mathbf{u}$ with $||\mathbf{u}|| = 1$ yielding:

$$\rho = ||\mathbf{x} - \mathbf{x}_\bullet||\ ,\ \mathbf{u} = \frac{\mathbf{x} - \mathbf{x}_\bullet}{\rho}\ ,\ \frac{\partial\rho}{\partial\mathbf{x}} = \mathbf{u}\ ,\ \frac{\partial\mathbf{u}}{\partial\mathbf{x}} = \frac{\mathbf{I} - \mathbf{u}\,\mathbf{u}^T}{\rho}$$

Since the potential is harmonic, it is analytic (see $\mathcal{P}_3$ in appendix A) and we can thus formalize the fact that $\lim_{\mathbf{x}\to\mathbf{x}_\bullet\in\partial\bar{\mathcal{U}}} V(\mathbf{x}) = +\infty$ writing without loss of generality:

$$V(\mathbf{x}) = \frac{v(\mathbf{x})}{\rho^\alpha} + w(\mathbf{x})$$

for some $v(\mathbf{x})$, $w(\mathbf{x})$ which derivatives are bounded in a neighborhood of $\mathbf{x}_\bullet$ while $v(\mathbf{x}_\bullet) \neq 0$.

A straightforward derivation using derivation chain rules yields:

$$\Delta V(\mathbf{x}) = \frac{\Delta v(\mathbf{x})}{\rho^\alpha} - \frac{2\,\alpha}{\rho^{\alpha+1}}\,\frac{\partial v}{\partial\rho}(\mathbf{x}) + \frac{\alpha\,(\alpha+2-n)\,v(\mathbf{x})}{\rho^{\alpha+2}} + \Delta w(\mathbf{x})$$

Because $0 = \Delta V(\mathbf{x}) = \frac{\alpha\,(\alpha+2-n)\,v(\mathbf{x})}{\rho^{\alpha+2}} + o(\rho^{-(\alpha+1)})$ everywhere in a neighborhood of $\mathbf{x}_\bullet$, we must have $\alpha\,(\alpha+2-n)\,v(\mathbf{x}) = O(\rho^{\alpha+2})$ but this incompatible with the fact that $v(\mathbf{x}_\bullet) \neq 0$ unless $(\alpha+2-n) = 0$ so that $\alpha = n-2$ since $\alpha \neq 0$.

As a consequence, from (14), such a potential is always of the form $V(\mathbf{x}) = \mu_{\mathbf{x}_\bullet}(\mathbf{x})\,\Phi(\mathbf{x} - \mathbf{x}_\bullet) + w(\mathbf{x})$ with $\mu_{\mathbf{x}_\bullet}(\mathbf{x}) = \sigma_n\,(n-2)\,v(\mathbf{x})$.

Considering now each point $\mathbf{x}_\bullet \in \partial\mathcal{U}$ for which we must have $\lim_{\mathbf{x}\to\mathbf{x}_\bullet} V(\mathbf{x}) = \pm\infty$ thus verifies the previous condition (or its opposite) at each point $\mathbf{x}_\bullet$, the potential must thus be, from (5), of the form:

$$V(\mathbf{x}) = \mathcal{A}(\mathbf{x}) + \omega(\mathbf{x})$$

using the measure $\mu(\mathbf{x}) = \int_{\partial\mathcal{U}} \delta(\mathbf{x} - \mathbf{x}_\bullet)\,\mu_{\mathbf{x}_\bullet}(\mathbf{x})$, while $\omega(\mathbf{x})$ is an harmonic potential bounded in $\bar{\mathcal{U}}$.

A step further, using the Green formula (see $\mathcal{P}_6$ in appendix A) we can write

$$\begin{array}{rcl}\omega(\mathbf{x}) & = & -\int_{\partial\mathcal{U}} \varpi(\mathbf{x}_\bullet)\,\frac{\partial G}{\partial\nu}(\mathbf{x},\mathbf{x}_\bullet)\,d\mathbf{x}_\bullet \\ & = & \int_{\partial\mathcal{U}} \frac{\partial\omega}{\partial\nu}(\mathbf{x}_\bullet)\,\Phi(\mathbf{x}-\mathbf{x}_\bullet) - \varpi(\mathbf{x}_\bullet)\,\frac{\partial\Phi}{\partial\nu}(\mathbf{x}-\mathbf{x}_\bullet)\,d\mathbf{x}_\bullet\end{array}$$

for some summable function $\varpi(\mathbf{x}_\bullet)$ defining $\omega(\mathbf{x})$, while $G(\mathbf{x},\mathbf{x}_\bullet)$ is the Green function related to $\partial\mathcal{U}$.

From (5) and since $\Phi(\mathbf{x}-\mathbf{x}_\bullet) = o(||\mathbf{x}-\mathbf{x}_\bullet||^{-(n-2)})$:

$$\begin{array}{rcl}V(\mathbf{x}) & = & \int_{\partial\mathcal{U}} \left[\mu(\mathbf{x}_\bullet) + \frac{\partial\omega}{\partial\nu}(\mathbf{x}_\bullet)\right]\,\Phi(\mathbf{x}-\mathbf{x}_\bullet) - \varpi(\mathbf{x}_\bullet)\,\frac{\partial\Phi}{\partial\nu}(\mathbf{x}-\mathbf{x}_\bullet)\,d\mathbf{x}_\bullet \\ & = & -\varpi(\mathbf{x}_\bullet)\,\nu(\mathbf{x}_\bullet)^T\nabla\Phi(\mathbf{x}-\mathbf{x}_\bullet) + o(||\mathbf{x}-\mathbf{x}_\bullet||^{-(n-2)}) \\ & = & o(||\mathbf{x}-\mathbf{x}_\bullet||^{-(n-1)}) \text{ unless } \varpi(\mathbf{x}_\bullet) = 0\end{array}$$

This last equality would be in contradiction with the form

$$V(\mathbf{x}) = \mu_{\mathbf{x}_\bullet}(\mathbf{x})\,\Phi(\mathbf{x}-\mathbf{x}_\bullet) + w(\mathbf{x}) = o(||\mathbf{x}-\mathbf{x}_\bullet||^{-(n-2)})$$

obtained previously so that we must state $\varpi(\mathbf{x}_\bullet) = 0$ for all $\mathbf{x}_\bullet$ yielding $\omega(\mathbf{x}) = 0$.

As a consequence $V(\mathbf{x}) = \mathcal{A}(\mathbf{x})$, adelicians defining the family of solutions of the present problem.

Local influence of the obstacles: about the 2D case

As illustrated in Fig. 3, the function $\Phi()$, for $n > 2$, has a "local" influence in the sense that

$$\lim_{||\mathbf{x}||\to+\infty}\Phi(\mathbf{x}) = 0$$

Its influence, for large values of $||\mathbf{x}||$, becomes negligible. The consequence is that the term $\mathcal{A}_i(\mathbf{x})$ related to the ith obstacle has a "local" influence on the potential value, which is a suitable property.

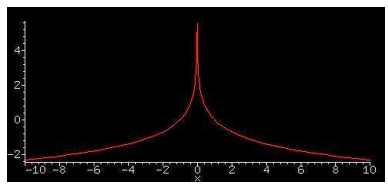

Figure 3: Profile of the function $\Phi()$ for $n > 2$.

On the other hand, in the 2D case, adelicians are still solutions of the proposed problem (although it is not clear if they are the only solution), but $\Phi(\mathbf{x}) = -\frac{1}{\sigma_2}\log(||\mathbf{x}||)$ with $\lim_{||\mathbf{x}||\to+\infty}\Phi(\mathbf{x}) = -\infty$. As a consequence, spurious influences of the obstacles at large distances are induced and caveats are to be expected when using this approach.

Hopefully, this is not a problem in practice, because any 2D problem can obviously be embedded in a 3D problem where the 3rd variable is set to 0 (geometrically, this corresponds to have cylindrical obstacles, which basis is the 2D original obstacle). We thus never used a potential with $n = 2$ in our application, even if the state is of dimension two, but still apply the ideas proposed here, using the previous trick.

Global influence of the goal: balanced adelician

Contrary to constraints/obstacles influence, the goal attraction must have a global influence in order the trajectory to be generated from any remote point. This clear separation between goal location influence and other loci influences is likely at the origin of the fact they seem to be represented in different maps of the brain, as reviewed previously.

At a formal level, the goal influence never vanishes but at a numerical level, its contribution may becomes negligible in (5). However, this global influence is obvious to maintain by *separating the constraints and the goal contributions* in (5) and by adjusting the relative weigth between the goal attraction and the obstacle repulsion. Here, we simply balance both contributions:

$$\int_{\partial\mathcal{U}_0}\mu_0(\mathbf{y})\,d\mathbf{y} = \sum_{i=1}^{r}\int_{\partial\mathcal{U}_i}\mu_i(\mathbf{y})\,d\mathbf{y}$$

For a punctual goal $\mathbf{x}_\infty$ this entirely defines the goal weight

$$\mu_0(\mathbf{x}_\infty) = \sum_{i=1}^{r}\int_{\partial\mathcal{U}_i}\mu_i(\mathbf{y})\,d\mathbf{y}$$

Bounded potentials related to an adelician

The present development is not restricted to an unbounded function $V(\mathbf{x}) = \int_{\partial\mathcal{U}} \Phi(\mathbf{x} - \mathbf{y})\, \mu(\mathbf{y})\, d\mathbf{y}$ because given any bounded bijective transformation, a simple change of variables allows to use a bounded representation (see [32] for details). Thanks to such a change of variable, a large family of (non-harmonic) potential are easily related to an adelician, allowing this approach to be quite general and very plausible to rely to a biological map activity.

More precisely, given any bounded transformation

$$\mu : \mathbf{x} \in \mathcal{R}^n \times V \in \mathcal{R} \rightarrow [a, b] \subset \mathcal{R}$$

bijective with respect to V at each $\mathbf{x}$, the related bounded potential

$$U(\mathbf{x}) = \mu(\mathbf{x}, V(\mathbf{x})) \text{ (thus } V(\mathbf{x}) = \mu^{-1}(\mathbf{x}, U(\mathbf{x})))$$

can be considered. This is a simple change of variables. From (1), the trajectory is directly generated using $\nabla U(\mathbf{x})$:

$$\gamma'(t) = -\left[\left[\nabla U - \frac{\partial\mu}{\partial\mathbf{x}}\right] / \frac{\partial\mu}{\partial V}\right](\gamma(t))$$

and:

$$\nabla U = \frac{\partial\mu}{\partial\mathbf{x}} + \frac{\partial\mu}{\partial V} \int_{\partial\mathcal{U}} \nabla\Phi(\mathbf{x} - \mathbf{y})\, \mu(\mathbf{y})\, d\mathbf{y}$$

is directly constructed from the adelician representation inside $\mathcal{U}$, while $\lim_{\mathbf{x}\rightarrow\partial\mathcal{U}} U(\mathbf{x}) = \lim_{V\rightarrow\pm\infty} \mu(\mathbf{x}, V)$ remains bounded.

For instance, it is straightforward to define, say:

$$U(\mathbf{x}) = \frac{1}{1 + e^{-V(\mathbf{x})}} \Leftrightarrow V(\mathbf{x}) = \log\left(\frac{U(\mathbf{x})}{1 - U(\mathbf{x})}\right) \tag{7}$$

with $U(\mathbf{x}) \in [0, 1]$ while conditions $\mathcal{C}_0$, $\mathcal{C}_i$ and $\mathcal{C}_c$ write:

$$\begin{array}{l} \lim_{\mathbf{x}\rightarrow\partial\mathcal{U}_0} U(\mathbf{x}) = 0 \text{ and } \forall i, \lim_{\mathbf{x}\rightarrow\partial\mathcal{U}_i} U(\mathbf{x}) = 1 \\ \forall \mathbf{x} \in \mathcal{U}, U(\mathbf{x})(1 - U(\mathbf{x}))\, \Delta U(\mathbf{x}) + (2\, U(\mathbf{x}) - 1)\, ||\nabla U(\mathbf{x})||^2 = 0 \end{array}$$

using $\gamma'(t) = -\frac{\nabla U(\gamma(t))}{U(\gamma(t))\,(1 - U(\gamma(t)))}$ to define the trajectory, as the reader can easily verify.

Such a bounded potential verifies a heavy non-linear elliptic partial differential equation obvious to derive:

$$\Delta U = \text{trace}(\frac{\partial^2\mu}{\partial\mathbf{x}^2}) + \frac{\partial^2\mu}{\partial V^2} / \left(\frac{\partial\mu}{\partial V}\right)^2 \left|\left|\nabla U - \frac{\partial\mu}{\partial\mathbf{x}}\right|\right|^2$$

and hopefully useless because never to be solved.

From adelician to locus maps

The previous definition (5) not only provides a general solution for $\mathcal{C}_0$, $\mathcal{C}_i$ and $\mathcal{C}_c$ but also provides a *representation* of the map where the trajectory has to be defined. If the trajectory generation problem is entirely defined (goal and constraints) the canonical solution (6) relates the trajectory map (defined by the goal definition $c_0(\mathbf{x}) \leq 0$ and constraint equations $c_i(\mathbf{x}) > 0$) with the potential.

Sparse versus dense representation

There is however a problem at the implementation level: how to approximate the integral by a finite summation ? This is a problem for both a computer implementation or a neural network biological implementation because of the curse of dimensionality.

More precisely, the ensemble of hippocampal place cells covers the 2D environment in a fairly dense manner, but since the number of neuronal unit is finite this is still a sparse representation. When considering higher-dimensional spaces the representation is indeed very sparse[4].

Trajectory or planning problems involves several degrees of freedom, and the size of a numerical tessellation of the parametric space increases as an exponential function of the problem dimension, event "a lot of" neurons (organized in a -indeed- dense but only 2D/3D map) would fail to correctly sample a representation in a higher dimensional space. Summarizing: *any relevant representation must be a* **sparse** *representation.* In our case this simply means considering adelicians with a sparse discrete measure:

$$\mathcal{A}_i(\mathbf{x}) = \sum_{\mathbf{y}_{ij} \in \partial \mathcal{U}_i} \mu_{\mathbf{y}_{ij}} \, \Phi(\mathbf{x} - \mathbf{y}_{ij}) \tag{8}$$

where only a "small" finite number of values $\mu_{\mathbf{y}_{ij}}$ of the measures $\mu_i()$ are to be taken into account, the other values being zero

Considering such a sparse representation, we have to be sure to generate a trajectory with obstacle avoidance, despite the fact the sampling is sparse. One simple idea is to remark that a collision with an obstacle indeed always occurs with the closest point of this obstacle, so that if the closest point is always introduced in the adelician the obstacle/constraint, repulsion with respect to this closest point should always avoid attaining the obstacle/constraint.

If this closest obstacle closest point rule is not taken into account, there is always a possibility of collision if the trajectory get very close to the obstacle.

This closest obstacle closest point rule is to be understood as a "minimal requirement" but there is obviously no problem to add more points to the representation, if available. Parsimony is crucial for a computer implementation, less important for a biological one.

This rule has a very important consequence: the sparse representation is not fixed but must adapted to the trajectory, as discussed in the next sub-section.

By doing this, we only generate a set of points which cardinal has the order of magnitude of the trajectory length without a direct dependence with respect to space dimension, except in the *worst case* where the space has to be entirely explored before finding a solution. This worst-case corresponds to an entirely congestioned state-space where the trajectory entirely explores the whole multi-dimensional space before attaining the goal. This is almost never encountered.

[4]There are, say, about $10^{6..8}$ locus cells in such a map. If a six degrees of freedom quantity is represented (i.e. representing a rigid position and orientation) this gives in each dimensional range only about .. 10 samples! This *is* sparse.

More precisely, with the proposed mechanism, each component creates a small "ball of repulsion". As such, the obstacle is seen as a "set of spherical balls": remote obstacles or obstacles without strong interaction are simply viewed as (almost) spherical shapes since the different projections of the trajectory will be almost equal at high distance. As soon as getting closer (or paying more "attention") to the obstacle, its shape is approximated in better details and not isotropic anymore.

Adaptive representation

A step ahead, in addition to the fact sparse representation must adapt to the trajectory, a trajectory problem is very seldom entirely defined: *obstacles/constraints are discovered during the trajectory generation.* In other words, the adelician representation (here the $(\mathbf{y}_{ij}, \mu_{\mathbf{y}_{ij}})$ values) is to be constructed during the "exploration". In our context, this is a very easy job: as soon as a new obstacle/constraint is "visible" we can add some related values and **adapt** the adelician, i.e. choose another adelician in the adelician's family taking the new information into account: this explains why it was so important not to a define "one" solution but a family. A trajectory generated by such a series of adelicians will not strictly corresponds to a trajectory defined such a potential, whereas some "exploratory" phases (i.e. a portion of trajectory may finally allow to discover a new obstacle/constraint thus backtrack taking this new element into account) are expected.

Considering such an adaptive representation, we have to be sure to generate a trajectory towards the goal, not an indefinite wandering trajectory. Convergence is obtained by the fact we have a finite number of compact obstacles, thus covered by a finite number of points for a sparse representation with a minimal distance ϵ between the covering points, formally:

$$\forall_{ij,\ i'j'} ||\mathbf{y}_{ij} - \mathbf{y}_{i'j'}|| > \epsilon \tag{9}$$

As a consequence, the related series of adelicians can not indefinitely increase because it is bounded, thus converges towards a limit. In the worst case, this limit is a complete sparse knowledge of the map representation.

The minimal distance ϵ must not be higher than the distance between obstacles and the minimal distance between the trajectory and the obstacles, thus has the order of magnitude of the system size. The higher ϵ the smaller the number of points. We are going to verify that this parameter is not critical.

Limiting the increase in terms of data points thanks to the use of sparse representation not only allows to save memory space and computation time but also limit the variations of the potential during adaptation. This stabilizes the trajectory generation process.

Sensori-motor loop embedding

This adaptive aspect has another consequence: the trajectory generation is not a blind open-loop process but is embedded in a sensory-motor loop. We thus have to formalize such a loop in order to understand the global behavior of the mechanism.

Here we consider a so called look-and-move paradigm where the next sensory input $\mathbf{x}(t+1)$ corresponds to the previous motor command $\mathbf{m}(t)$ taking a bounded uncertainty ν_t into account:

$$\mathbf{x}(t+1) = \mathbf{x}(t) + k\ [\mathbf{m}(t) + \nu_t]\ \ , k > 0\ , ||\nu_t||_{\mathbf{\Lambda}} < \rho \tag{10}$$

where ρ is the bounded uncertainty maximal value and k the motor-command gain control.

Here ν_t is an uncorrelated bounded random perturbation with $E[\nu_t] = 0$ (the "noise" of the motor-sensory loop). The choice of a bounded error is due to the fact we do not want to *likely* avoid obstacles but *always* do it. The value of the metric $\mathbf{\Lambda}$ is specified assuming that it is possible to define for each parameter an "error" i.e. a maximal value of variation below which the error is bounded (see [16, 33] for a general discussion), e.g. 1 mm for a distance measured by hand, 1 pixel of measure related to an image, etc.. Up to a change of variable $\mathbf{x} \rightarrow \mathbf{\Lambda}^{\frac{1}{2}}\,\mathbf{x}$ we can state $\mathbf{\Lambda} = 1$ in the sequel without loss of generality.

Since, from (1), we only define the trajectory direction (being a 1st order descent algorithm) not its magnitude, we thus have to introduce a motor command gain adjusted by the control algorithm to properly defined the motor command $\mathbf{m}(t) = -\nabla V(\mathbf{x}(t))$. It is clear that the distance between the trajectory and the obstacles must always be higher that $k\,\rho$ in order to avoid a collision due to the motor-command uncertainty. This motor-gain has also to be adjusted depending on the dynamic of the motor-loop (the higher the phase lag, the smaller the gain maximal value), which is out of the scope of the present development: here, we are going to propose a bound for this gain and consider that its adjustment is another problem, depending on the motor-loop implementation.

Choosing a step by step motor command may seems restrictive but is a reasonable choice regarding trajectory generation because robotic continuous control loops are not defined at this level, but use trajectory generation as input [19, 1, 9]. Such separation between "planning" and "reflex" is also present in biological systems.

Goal-directed versus exploratory navigation

By default, the goal is known to the agent from the beginning, while obstacles are unknown to the agent. Goal directed experiment corresponds to the situation where the target can be smelled, seen or eared. This seems in contrast to, e.g., exploratory experiments (e.g. in the Morris Water Maze where the rat has to learn to find the goal).

However, the same formalism is directly restricted to a situation where the goal is unknown (no attractive term), the exploration being only realized by obstacle repulsion.

It also applicable in situations with intermediate goals or where the goal is diffuse (weak attraction over a large area).

Defining such a non punctual potential is straightforward in this framework using a constraint of the form $c_0() < 0$. As soon as the goal is almost attained it has to removed from the potential (in order to avoid unbounded values). This, in fact, introduces a canonical mechanism to take an intermediate sub-goal into account: adding it to the potential and removing it when attained.

Similarly the goal is not necessarily attractive from the beginning but only as soon as visible. This obviously fits in the present mechanism.

This is very likely what is observed in a biological locus map where a rather dense set of attained loci are represented (and inhibited when attained).

Introducing several intermediate sub-goals also allows to introduce a higher-level control, for instance specifying a trajectory at a coarse scale or generating repetitive motions (see e.g. [6]).

This versatile capabilities are illustrated in the experimental session.

Comparison with biological locus-maps

As being defined by an un-ordered locus list $\{\cdots(\mu_{\mathbf{y}_{ij}}, \mathbf{y}_{ij})\cdots\}$ a sparse adelician corresponds to a locus-map without any topographical constraints for the map where this information is registered: storing a new locus corresponds to recruiting a new site, retrieving a previous map corresponds to a simple retrieving of the locus list (in fact the convergence of neural map coding the loci towards an attractor corresponding to the previous list). Here a neural site of the locus list corresponds to a given index ij and can be reused when another map is taken into account.

The weights $\mu_{\mathbf{y}_{ij}}$ may play an important role to adjust/optimize the representation. They correspond to the output weight of each locus cell when combined to build a local shift. However, since we do not have precise information about how they could be determined in a biological context, we simply consider $\mu_{\mathbf{y}_{ij}} = 1$ (Occam razor principle) to avoid non pertinent parameters in the computational model.

As stressed before, in the hippocampus, not only the closest obstacle closest point is introduced in the locus map, whereas other locus perceived by the subject can be added. However, the fact proximal points have to be registered is an important feature, coherent with actual biological findings and if this is not the case, the present model would be questionable. Here "proximal" does not mean that the exact Euclidean projection onto the nearest obstacle as to calculated by the biological structure: the requirement is simply to locate the obstacle contact point which is known as a reliable cue (e.g. [18]).

A step further, separation between goal attraction and obstacle repulsion is easy to design, combining the two map outputs to generate the motor signal, as it is now often assumed to be the case.

Another very important point is that in both cases, loci are added but not deleted to the map, as discussed in the sequel. Removal of biological locus-cell activity seems not to have been observed *during* the navigation in a given spatial map. This is a crucial point, coherent with actual data and if this is not the case, the present model would be questionable.

Similarly, the elongated versus isotropic nature of the locus-map depends on the fact it corresponds to a border of the domain (thus an obstacle) or not (thus an intermediate goal), is in coherence between the computational model and the biological data, as discussed previously.

In both cases (computational and biological models), the mechanism output is a location shift. In the computational model it is related to the gradient of the locus-map activity. The

corresponding projections CA3 → CA1 are likely to perform such a partial differentiation [2] of the locus map activity.

In both cases also, loci are specified in a spatial frame of reference and in both cases too, loci sizes of influence has the order of magnitude of (and is higher than) the subject size.

A step further, in both cases, beacon navigation is easily specified by defining sub-goals and then interchanging the goal (a previous goal could also optionally becomes an obstacles when reached driving the system towards the next goal). Similarly "wandering" behavior simply corresponds to goal evanescence. A step ahead, several goals may compete (the $\mathcal{U}_0$ set could be easily defined as two different connected components), the subject being attracted by both targets and the choice being driven by the present mechanism.

Summarizing, the present computational model seems really compatible with what is yet understood regarding the underlying biological mechanisms. It however requires specific assumptions which may be contradicted (or not) by further investigations. In any case it does not provide a detailed description of the biological structures mechanisms (such models already exist, e.g. [25]) but simply fill one gap and shows how such local mechanisms solve the global problem, as verified now.

Another harmonic function approach to modeling striatal function has been already proposed [5, 6]. The framework allows to realize both discrete and repetitive motions. It is however limited to 2D motions for computational limitations reviewed here. Striatal neurons are viewed as modules that compute potential functions responsible for guided movements and implements coordinates transformations to various configuration spaces [5]. The model proposes that resistive coupling among striatal neurons give rise to harmonic potential functions (expressed as an ensemble of neuronal membrane potentials). In thalamic formations the underlying diffusion process is likely not performed at this level but directly related to the neural map connections which can implement such computational mechanisms [11, 31].

Convergence of closed loops with sparse adaptive adelicians

Let us write $\pi_{\mathcal{S}}(\mathbf{x})$ the projection[5] of $\mathbf{x}$ onto a set $\mathcal{S}$ and $d(\mathbf{x},\mathcal{S}) = ||\mathbf{x} - \pi_{\mathcal{S}}(\mathbf{x})||$ the distance between $\mathbf{x}$ and $\mathcal{S}$. We also consider, say, the ϵ-projection onto an obstacle:

$$\pi^{\epsilon}_{\partial\mathcal{U}_i}(\mathbf{x}) = \begin{cases} \mathbf{y}_{ij} \in \partial\mathcal{U}_i & \text{if } ||\mathbf{y}_{ij} - \pi_{\partial\mathcal{U}_i}(\mathbf{x})|| < \epsilon \\ \pi_{\partial\mathcal{U}_i}(\mathbf{x}) & \text{otherwise} \end{cases}$$

$\mathbf{y}_{ij}$ being a point in the sparse representation. With this approximate projection the distance is approximated up to ϵ, i.e.:

$$d(\mathbf{x},\pi_{\partial\mathcal{U}_i}(\mathbf{x})) + \epsilon \geq d^{\epsilon}(\mathbf{x},\partial\mathcal{U}_i) \geq |d(\mathbf{x},\pi_{\partial\mathcal{U}_i}(\mathbf{x})) - \epsilon|$$

writing $d^{\epsilon}(\mathbf{x},\partial\mathcal{U}_i) = d(\mathbf{x},\pi^{\epsilon}_{\partial\mathcal{U}_i}(\mathbf{x}))$.

Using these notations, the previous discussion is formalized by the following result: **given an initial position and adelician**

$$\gamma(0) \textbf{ with } d(\gamma(0),\cup_{i=1}^{r}\partial\mathcal{U}_i) > 0 \textbf{ while } V_t(\mathbf{x}) = 0$$

the following series (writing $i_t = \arg\min_i d(\gamma(t),\partial\mathcal{U}_i)$ **):**

$$\begin{array}{rcl} \gamma(t+1) & = & \gamma(t) + k\,\left[-\nabla V_{t+1}(\gamma(t)) + \nu_t\right]\ ,\ ||\nu_t|| < \rho \\ V_{t+1}(\mathbf{x}) & = & V_t(\mathbf{x}) + \mu_{i_t\,t}\left[\Phi(\mathbf{x} - \pi^{\epsilon}_{\partial\mathcal{U}_{i_t}}(\gamma(t))) - \Phi(\mathbf{x} - \pi^{\epsilon}_{\partial\mathcal{U}_0}(\gamma(t)))\right] \end{array} \tag{11}$$

verifies (i) $\forall t > 0, d(\gamma(t),\cup_{i=1}^{r}\partial\mathcal{U}_i) > 0$ **and** (ii) $\lim_{t\to+\infty} d(\gamma(t),\mathcal{U}_0) = 0$ **as soon as** k **is small enough with** $\mu_{i_t\,t} \in \{0,1\}$ **and** $P\{\mu_{i_t\,t} = 1\} > 0$**.**

The formula $\lim_{t\to+\infty} d(\gamma(t),\mathcal{U}_0) = 0$ does not mean convergence occurs at infinity. As soon as the distance to the goal is smaller than the distance to the closest obstacle, it is clear that a straight-line allows to attain the goal and the problem is solved. In other words $d(\gamma(T),\mathcal{U}_0) < \rho$ for some finite value $T < +\infty$.

Writing $P\{\mu_{i_t\,t} = 1\} > 0$ means to set $\mu_{i_t\,t} = 1$ but not necessarily at each step. Here, we simply stress the fact there are only very weak constraints on how to increment an adelician. Adding a weight to the adelician at each step corresponds to $P\{\mu_{i_t\,t} = 1\} = 1$.

Conditions derived now are sufficient conditions. They have been chosen in order to generate a "minimal" adelician (as sparse as possible). Several alternatives are possible, as evoked previously. Here the idea is to show that it works even for a very sparse adelician.

[5] *About projection calculation.* Here, we have to compute the projection $\mathbf{x}_{i\,t}$ of $\mathbf{x}_t$ onto $\partial\mathcal{U}_i = \{\mathbf{x}, c_i(\mathbf{x}) = 0\}$.
Such a point is defined by the following Lagrangian formulation:

$$\mathbf{x}_{i\,t} = \arg\min_{\mathbf{x}}\max_{\lambda} \tfrac{1}{2}\,||\mathbf{x} - \mathbf{x}_t||^2 + \lambda\, c_i(\mathbf{x})$$

which, from the related normal equations, is easily solved (see [34] for a complete development in a more general case) by an algorithm of the form:

$$\mathbf{x}^{n+1} = \alpha\left[\mathbf{x}_t + \mathbf{g}^n\ \left[\mathbf{g}^{n\,T}(\mathbf{x}^n - \mathbf{x}_t) - c_i(\mathbf{x}^n)\right]\right] + (1-\alpha)\,\mathbf{x}^n$$

with $\mathbf{g}^n = \nabla c_i(\mathbf{x}^n)/||\nabla c_i(\mathbf{x}^n)||$ starting from $\mathbf{x}^0 = \mathbf{x}_t$ or using a previous estimate $\mathbf{x}_t$ of this projection. In the implementation proposed in [34] choosing among $\alpha = 1, \frac{1}{2}, \frac{1}{4} \cdots \frac{1}{2^p}$ the highest value such that $||c_i(\mathbf{x}^{n+1})|| \leq ||c_i(\mathbf{x}^n)||$ it has been shown that the series is always convergent. This series converges towards the solution as soon as the second order derivative $\nabla^2 c_i$ is bounded and the equation is not singular, i.e. $||\nabla c_i(\mathbf{x}^n)|| \neq 0$.
It is established that when sufficiently close to the obstacle (which is always the case in our context), even for concave obstacles, convergence occurs [35]. Otherwise, it converges toward a wrong but approximate value.

(i) In order to show that $\forall t > 0, d(\gamma(t), \cup_{i=1}^{r} \partial\mathcal{U}_i) > \rho$,
let us assume by induction that for some $t \geq 0$, $d(\gamma(t), \cup_{i=1}^{r} \partial\mathcal{U}_i) > \rho$.

In a ball of center $\gamma(t)$ and radius $||\mathbf{d}|| = d(\gamma(t), \cup_{i=1}^{r} \partial\mathcal{U}_i) = ||\gamma(t) - \pi_{\partial\mathcal{U}_i}(\gamma(t))||$, $\mathbf{d} = \gamma(t) - \pi$, $\pi = \pi_{\partial\mathcal{U}_i}(\gamma(t))$ (in words the minimal distance to all obstacles is the minimal distance to the closest obstacle), there is no obstacle (since $\partial\mathcal{U}_{i_t}$ is the closest one). If we can maintain $\gamma(t+1)$ in such a ball, i.e. if $||\gamma(t+1) - \gamma(t)|| < ||\mathbf{d}||$ collisions are avoided, i.e. $d(\gamma(t+1), \cup_{i=1}^{r} \partial\mathcal{U}_i) > 0$ as represented here:

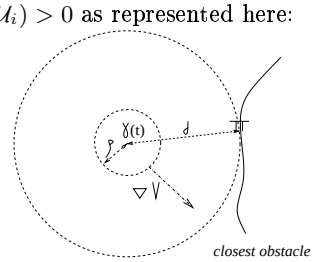

In fact, as soon as:

$$k < ||\gamma(t) - \pi_{\partial\mathcal{U}_i}(\gamma(t))|| / \left[||\nabla V_{t+1}(\gamma(t))|| + \rho\right] \tag{12}$$

we obtain $||\gamma(t+1) - \gamma(t)|| < k\ [||\nabla V_{t+1}(\gamma(t))|| + \rho] < ||\mathbf{d}||$ as required.

(ii) A step further, if the potential is stationary (i.e. $V(\mathbf{x}) = V_{t+1}(\mathbf{x}) = V_t(\mathbf{x})$)

$$\begin{aligned} &V(\gamma(t+1)) = V(\gamma(t) + k\ [-\nabla V(\gamma(t)) + \nu_t]) \\ &= \left[V + k[-\,||\nabla V||^2 + \nabla V^T \nu_t] + k^2/2\,(\nu_t - \nabla V)^T\, \nabla^2 V\,(\nu_t - \nabla V)\right. \\ &\left. + o(k^3)\right](\gamma(t)) \end{aligned}$$

and because the noise ν_t at time t is not correlated with $V(\gamma(t))$ which only depends on previous values, $E[\nabla V^T\, \nu_t] = 0$ and $E[\nabla V^T\, \nabla^2 V\, \nu_t] = 0$. Considering the value in average, i.e. its expectation, a few algebra yields:

$$\begin{aligned} &E[V(\gamma(t+1))] \\ &= E\left[V - k\,||\nabla V||^2 + k^2/2\,(||\nabla V||^2_{\nabla^2 V} + ||\nu_t||^2_{\nabla^2 V}) + o(k^3)\right](\gamma(t)) \end{aligned}$$

with $||\nu_t||^2_{\nabla^2 V} < \rho^2\, ||\nabla^2 V||$ so that as soon as:

$$k < 2\,||\nabla V||^2 / \left[||\nabla V||^2_{\nabla^2 V} + \rho^2\, ||\nabla^2 V||\right]$$

the 1st order term is higher that the second order term and as soon as k is small enough for the higher order terms to be negligible, the 1st order term is preponderant and we define a minimizer on this harmonic potential yielding $\lim_{t\to+\infty} d(\gamma(t), \mathcal{U}_0) = 0$, as already discussed.

If the potential is not stationary, because $P\{\mu_{i_t\, t} = 1\} > 0$, it defines an increasing bounded series, thus with a maximal element which is a stationary harmonic potential yielding convergence too.

The formula $i_t = \arg\min_i d(\gamma(t), \partial\mathcal{U}_i)$ does not require to calculate all distances to all obstacles since from a previous estimate of the distance $d(\gamma(t-n), \partial\mathcal{U}_i)$ the distance to remote obstacles can be bounded

$$d(\gamma(t), \partial\mathcal{U}_i) > |d(\gamma(t-n), \partial\mathcal{U}_i) - d(\gamma(t-n), \gamma(t))|$$

only a few distances have to be updated.

The gain k is bounded to guaranty the potential decrease (if the potential does not decrease a simple efficent rule is to divide it for the next step) and also *strictly* bounded by (12) to avoid any collision.

It however remains freely adjustable in this double range: effect of such an adjustment is discussed previously and experimented in the sequel. In biological systems, such an adjustment is likely related to other cortical areas involved in motivation, global task control, etc..

3 Experimenting trajectory generation

We experiment different aspects of the proposed method implementing the following algorithm:

Initialization Detect if the problem is well posed, i.e. if the goal and the initial point verify the constraints.

Iteration From the current point:

- identify the closest obstacle and calculate the closest point on it,
- eventually update the harmonic potential function,
- calculate the new trajectory point,

as detailed in (11) and (12) and adding a weight to the adelician at each step.

Termination When the goal is attained.

Except in Fig. 5 we use an intermediate value of k for the motor gain (half the maximal value).

Interactive 2D demonstration

A toy experiment[6] is used to validate and evaluate the process. We propose this simulation in 2D (using the 2D "trick" introduced previously) to have a better view of the algorithm behavior. In order to study an almost "worst" case where block-up situation may occur, we experiment our method in a labyrinth simulation of small dimensions in order to maximize the "congestion".

A first result, shown in Fig 4, clearly illustrates how the mechanism explores the admissible space at the same time as the trajectory is generated.

We have experimentally observed, qualitatively, a two phases trajectory generation:

(1) an "exploratory" phase where the trajectory is somehow erratic but where the harmonic potential is highly adapted and

(2) a fast "displacement" phase where the trajectory is smooth and directed either towards the final goal or towards an intermediate location where an exploratory phase restarts.

This "exploratory" behavior is re-enforced by the fact that the trajectory tends to add repulsions with respect to close (parts of) obstacles, during the next steps, the tendency is

[6] Available at `http://www-sop.inria.fr/odyssee/research/vieville-vadot:02`

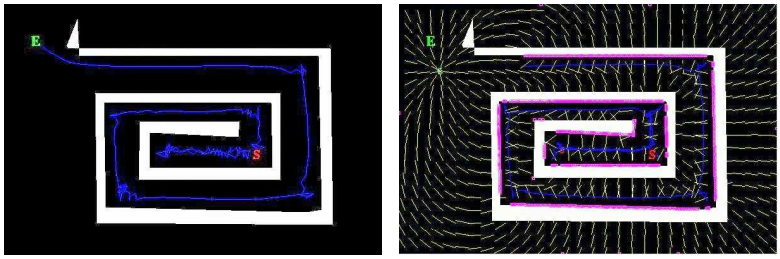

Figure 4: Showing the behavior of the mechanism in a "labyrinth" experiment. In the *left* view, the trajectory is starting at S and ending at E. At the beginning, attracted by the goal the trajectory starts in the wrong direction; then, because of obstacle repulsion, it finds its way out. At each change of direction, some trials are required to obtain a correct repulsion in order to be driven towards the goal. In the *right* view, "control" points onto the obstacle (in *magenta*) and the potential field gradients (in *yellow*) are drawn. The potential field has indeed no singularity except on the goal. We observe that a minimal number of points, i.e. the closest point to the obstacle, are used.

not for the trajectory to re-generate the same segment but to be pushed by the repulsion component elsewhere.

This exploratory mechanism is indirectly under the control for the motor "gain" parameter, leading to several "strategy" of exploration as illustrated in Fig. 6.

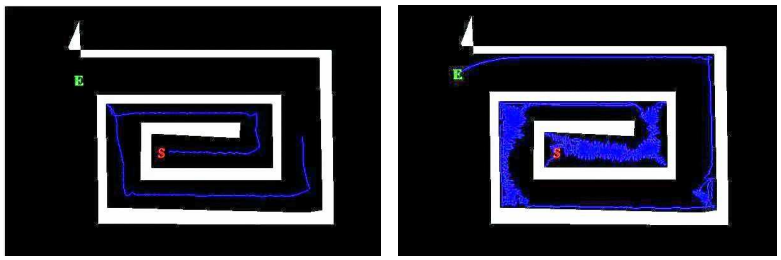

Figure 5: Showing the behavior of the mechanism with different motor-control gain. In the *left* view the motor gain is minimal yielding infinitesimal displacements from one step to another; the trajectory is thus smoother but convergence is slower (for the same number of iteration the system has not completed its task). In this configuration the trajectory is in the middle of the track between two obstacles, since adding a repulsion with respect to the closest obstacle point tends to balance the obstacles influence. In the *right* view the motor response is maximal yielding a "jump on obstacle" strategy: this "exploratory" behavior generates an erratic trajectory, in average along obstacles.

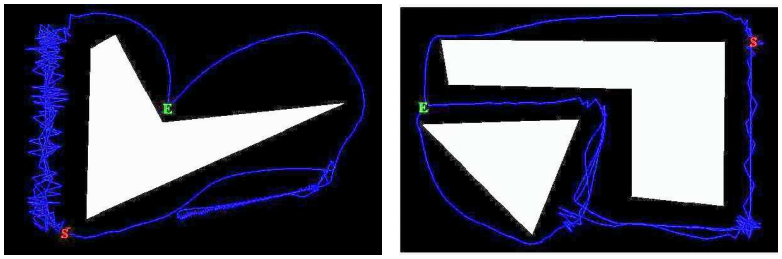

Figure 6: Showing the behavior of the mechanism with different trials. In the *left* view, the 1st run is erratic and yields a lot of exploration before finding a solution (the left-top trajectory) towards the goal. When rerun (the bottom right trajectory) the mechanism avoid re-doing the exploration and uses another way. Note that, because of the obstacle acute angle edge the bottom trajectory "hesitates"and then turn around it. In the *right* view, three successive trajectories are shown: the 1st finds a way between the two obstacles, with a few "for/back-ward" exploration; the 2nd is smoother and explore another way (the far bottom one), because of the repulsion left by the 1st exploration; the 3rd (the upward trajectory) starts towards another direction and find yet another (here shorter) way.

Although, geometrically, the trajectory may be used "backward" i.e. from the goal to initial point, in practice the proposed mechanism has a very skew-symmetric behavior as illustrated in Fig. 7.

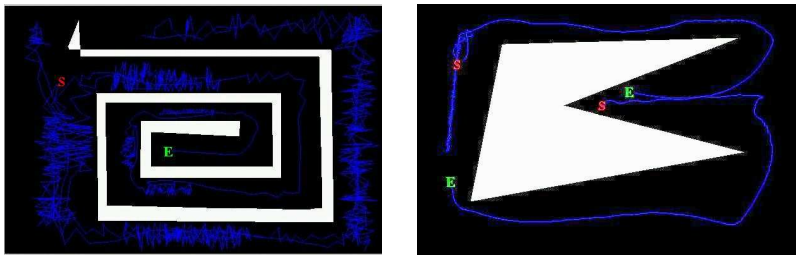

Figure 7: Showing the skew-symmetry between start and end points. In the *left* view, when the end point is inside the labyrinth, the mechanism may 1st explore all around before finding enough repulsion in order to enter the labyrinth and find its way. Even in this case, the behavior is much more erratic than in the symmetric situation shown in Fig. 4. In the *right* view, this skew-symmetric behavior is illustrated by a much simpler problem, for which it is still easier to, roughly speaking, get out of a "trap" than to get in.

In the present model, we have experimented it is very important to *never remove previously added points* allowing to always have a *different* value of the potential thus never

"loop forever" i.e. redo the same thing. We have explicitly experimented that trying to save memory space and computation time by removing points (even smoothly .. partially .. etc..) always generates periodic (thus non-convergent) trajectories in congested situations.

A step further, we have experimented if the use of an adelician may be extended to different paradigms of trajectory generation, as reported in Fig. 8: extensions may include the case where the potential function already represents the full geometry of the environment or where an "agent" can observe its environment, adding locations in the "line of sight". We have simulated this last situation by simply adding projections on obstacles along the direction of the displacement (considered as the "gaze direction"). This is a rough approximation, but a more precise mechanism depends on the way (camera ? other sensor ?) the observer can input data from its environment. Here the goal was simply to suggest, as a perspective of the present work, that we could use the method in several sensory-motor interaction schemes.

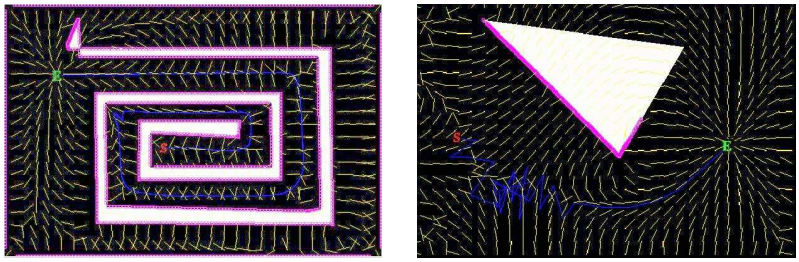

Figure 8: Showing how the method may be adapted to different strategies. In the *left* view, we have considered a case where the potential function already represents the full geometry of the environment: in that case the algorithm does not modify the potential, while we obtain a smoother trajectory in the "median way". In the *right* view, we have considered adding spread of boundary locations within the "line of sight" (see text for details): the method still works in this case.

In terms of optimality, as illustrated in the left view of Fig. 9, the mechanism does not look for the "shortest" but -in a sense- the "safest" trajectory since, with a small gain, it always generate a repulsion with respect to the closest obstacle.

Using the same mechanism for other behaviors.

A step ahead, we illustrate how the same mechanism (or a very small variant) is able to generate different kind of behaviors. In Fig. 10 we have introduce several goals as it is very likely the case in a biological loci-map. We observe that the mechanism still works, and that a large number of goals does not impair the original behavior. More than that, introducing intermediate goals can help to generate suitable trajectories.

Yet another step ahead, when no goal, we observe a wandering behavior, with a large exploration of the space, for the simple reason that as soon as an obstacle has been detected,

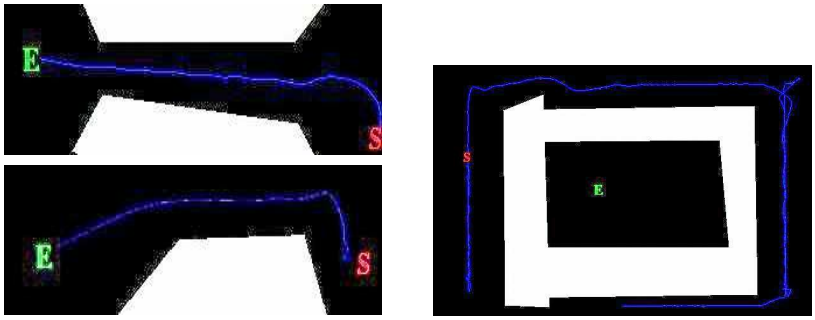

Figure 9: Showing additional properties of the mechanism. In the *left* views, as discussed for Fig. 6, with a small gain, the mechanism tends to travel in the middle between obstacles. In the *right* view, there is NO solution the present implementation .. loops forever .. turning around to try to find a way. At higher level, this caveat is easily avoided.

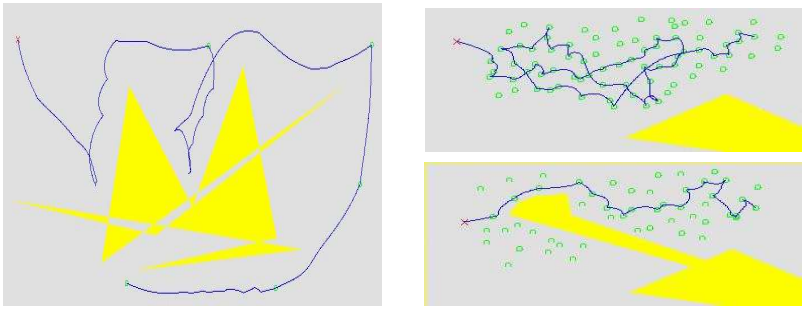

Figure 10: Showing how to use a simple variant of this mechanism for a goal directed exploration. Here, not one, but many goals have been introduced in the potential with the simple rule that the contribution is inhibited when the intermediate is attained. In the *left* view, it is shown how the trajectory is automatically generated from one intermediate goal to another. In the *right* views, a rather dense set of intermediate goals has been introduced, showing how the exploration is realized, taking not all but a sub-set of goals into account and generating relevant trajectories regarding the exploration of the environment.

a repulsive element is introduced in the potential yielding the exploration of another part of the environment.

If the potential would have been non adaptive, but fixed, as being an harmonic potential the trajectory would have converged towards a unique minimal, in any. We have observed situations where this occurs: the trajectory not being closed to obstacles, there is only a

very little adaptation of the potential and convergence towards a unique global minimum is obseved.

Anyway, it is clear that without goal, the exploration of the environement remains poor. A proper exploration is driven by the occurence of several temporary goals, as discussed previously.

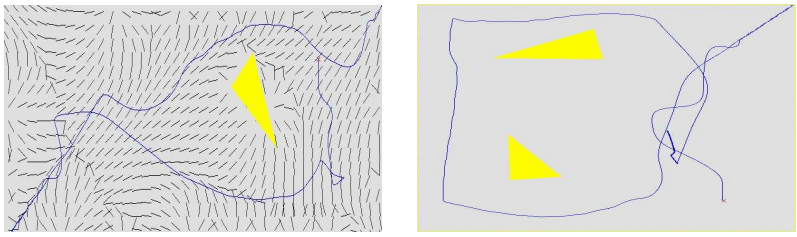

Figure 11: Showing how the same mechanism is used in the absence of any goal. As expected, a wandering behavior is generated. In the *left* view, the potential generated during the trajectory is shown, the geometry of the field is clearly induced by the geometry of the obstacles. In the *right* view, it is made visible that some parts of trajectory corresponds are straight and some are bended with several walk around the same position. These two qualititavive effects are directly related to the evolution of the potential.

Experimenting a high-dimensional problem

A step further, we have experimented our mechanism for a high-dimensional problem: a ten-degrees of freedom virtual 2D robotic arm is to be put up, from an initial "folded" position to a final "raised" position, as illustrated in the left part of Fig. 12. This set-up shows that the method still work in higher dimensions, as reported in the right part of Fig. 12. It must not be considered as a realistic "robotic" experiment.

Here the state-space corresponds to the ten angles of this virtual arm, this say "angular" state space is not Euclidean. This explains why when exploring this space we may obtain unexpected configurations as in Fig. 12. We have further illustrated the behavior of the algorithm in Fig. 13, showing a obstacle closest point in this state-space and also showing a more relevant trajectory, using an infinitesimal gain.

4 Conclusion

We have presented a model of trajectory generation based on harmonic potentials. The novelty of this work is to define a family of unbounded potentials, called adelicians, and derive a series of sparse adaptive potential incrementally built when the sensory-motor loop is acting.

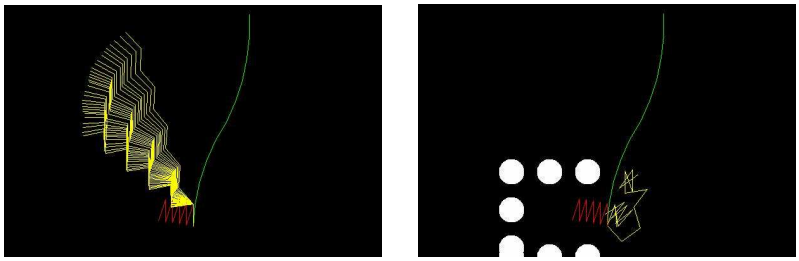

Figure 12: A ten-degrees of freedom virtual 2D robotic arm. In the *left* view, the robotic arm is put up from an initial folded position in red to a final raised position in green; only the middle part of this trivial trajectory is shown to figure out the set-up. In the *right* view, obstacles constraint the trajectory and a solution has to be found escaping from the "trap"; here only two intermediate positions (among about 20-30 steps) are shown in yellow to keep visibility, surprisingly some angles are tilted because, as in the 2D case, several configurations are explored in the angular state space along the trajectory.

Figure 13: Details about the trajectory generation. In the *left* view, for the same conditions, the magenta configuration corresponds to one "obstacle closest point" with respect to the initial position. The initial position is thus projected, in the angular state space, onto the closest configuration yielding a collision. This point is added as repulsive to the potential. In the *right* view, the trajectory has been generated with an infinitesimal gain, leading to a much more regular set of configurations. Here only the beginning of the trajectory until the robotic arm "escape from the trap" is shown.

As such, it is a solution to the problem of trajectory generation in high-dimensional state spaces: the high computation cost is avoided by considering such a sparse representation.

A step further, the set of points defining the adelician also defines a sparse spatial representation of the environment, based on locus-maps. How much such a computational model, biologically plausible, may help understanding the hippocampal related structures mechanisms ? As pointed out here, it only demonstrates that local "where-to-go-next" hippocampal mechanisms, if related to an adelician, also solves the global trajectory generation problem. This is much in favor of what is actually hypothesized regarding such biological mechanisms, whereas there is no need to assume any "supervisor" or mechanisms which complexity are an order of magnitude higher. The fact such locus-maps may not be localized in a unique structure but several and that the complete behavior is a result of the interaction

between such maps is a key issue. Further investigation should be conducted to analyze this biological plausibility. More complex behaviors may be represented by trajectory in an abstract state space.

A key aspect of the present model, is related to time: synaptic delays between sensory input and motor output in navigation are rather short, compatible with a sensory-motor as described here, but by no means with a "high-level planning algorithm´´. The fact the present model, which ambition is only to explain the phenomenology, respect these delays and facilitate robust navigation is likely its best argument of plausibility, at this preliminary stage.

Further technical development

An important issue is the generalization from the Euclidean space to non-linear manifolds. This technical issue is important for two reasons:
- for a robot or another mechanical system the physical parametric space is not always isomorphic to a unique compact (e.g. for 3D rotations with angles which may be higher that π) but has a more complex mathematical structure;
- cortical maps are intrinsically "curved space" (see e.g. [23]) with the fact that parametric spaces of dimension $n > 2$ (e.g. the visual areas which code retinal localization, edges orientation, binocular disparity, color .. in a "interlaced" way) are represented onto cortical maps.
This generalization to manifolds, although rather technical, should be relatively straightforward using so-called harmonic maps (defined by Beltrami equations).

A step further, we have mentioned that this formalism also allows to consider non-holonomic constraints [7], using not only Dirichlet but also Neumann constraints. Here the challenge is to obtain a generalization of the adelician with Neumann conditions. In the standard literature, it appears that it is not easy to obtain a "finite formula" in this case. A hope is that using unbounded potential like adelicians provides the same simplification as for Dirichlet conditions. This has to be checked carefully.

The present development proposes a restrictive mechanism to define the meta-parameters $\mu_{\mathbf{y}_{ij}}$ but several alternatives can be studied:
- the trajectory kinematic depends on the motor-command gain (related to the meta-parameters) which can be optimized in order to control the shape of the trajectory,
- the relative weight between goal attraction and obstacles repulsion, here balanced, is also tunable depending on the application,
- when a trajectory has been found, a next trajectory toward the same goal may simply re-used the same potential or attempt to smoothed it to obtain an optimized run,
- prior information about obstacle importance (e.g. "dangerosity") may be introduced by adjusting the meta-parameters and a known environment can easily be predefined with optimal meta-parameters,
- sub-goals are easily introduced to define complex planning tasks: tuning the meta-parameters obviously allow to shift from a part of the goal to another, either in sequence or in reaction to the subject behavior,

- when building an adelician, what is learned is not and must not be forgotten to guaranty the convergence; attempting to weaken this assumption may help reducing the size of the representation, or may be a requirement regarding biological plausibility.

Such ideas should improve the trajectory performance: length, smoothness, reproducibility, etc.. The present computational model is thus an apparently interesting but still preliminary attempt to develop trajectory generation based on adelicians.

References

[1] J. Barraquand and J. Latombe. On nonholonomic mobile robots and optimal maneuvering. *Revue d'Intelligence Artificielle*, 3, 1989.

[2] K. I. Blum and L. F. Abbott. A model of spatial map formation in the hippocampus of the rat. *Neural Comput.*, 8(1):85–93, 1996.

[3] J.-D. Boissonnat and M. I. Karavelas. On the combinatorial complexity of euclidean voronoi cells and convex hulls of d-dimensional spheres. Technical Report 4504, INRIA, July 2002.

[4] G. Bugmann, J. Taylor, and M. Denham. *Route finding by neural nets*, chapter Neural Networks, pages 217–230. Alfred Walter Ltd, Henley on Thames, 1995.

[5] C. Connolly and J. Burns. A new striatal model and its relationship to basal ganglia diseases. *Neuroscience Research*, 13:271–274, 1993.

[6] C. Connolly, J. Burns, and M. Jog. A dynamical-systems model for parkinson's disease. *Biol. Cybern.*, 83:47–59, 2000.

[7] C. Connolly and R. A. Grupen. Nonholonomic path planning using harmonic functions. Technical Report UM-CS-1994-50, UMass, 1994.

[8] C. I. Connolly. Harmonic functions and collision probabilities. *International Journal of Robotics Research*, 16(4):497–507, 1997.

[9] C. I. Connolly and R. A. Grupen. The applications of harmonic functions to robotic. *Journal of Robotic Systems*, 10(7):931–946, 1993.

[10] E. Coste-Maniere, L. Adhami, R. Severac-Bastide, A. Lobontiu, K. Salisbury, J. Boissonnat, N. Swarup, G. Guthart, E. Mousseaux, D. Blanchard, and A. Carpentier. Optimized port placement for the totally endoscopic coronary artery bypass grafting using the da vinci robotic system. In *International Symposium on Experimental Robotics*, Lecture Notes in Control and Information Sciences. Springer–Verlag, 2001. to appear.

[11] G.-H. Cottet and M. E. Ayyadi. A Volterra type model for image processing. *IEEE Transactions on Image Processing*, 7(3), Mar. 1998.

[12] H. Eichenbaum, P. Dudchenko, E. Wood, M. Shapiro, and H. Tanila. The hippocampus, memory and place cells: is it spatial memory or memory space ? *Neuron*, 23:209–226, 1999.

[13] L. Evans. *Partial Differential Equations*, volume 19 of *Graduate Studies in Mathematics*. Proceedings of the American Mathematical Society, 1998.

[14] P. J. Frey and H. Borouchaky. Geometric surface mesh optimization. *Computing and Visualization in Science*, 1:113–121, 1998.

[15] H. Frezza-Buet, N. Rougier, and F. Alexandre. Integration of biologically inspired temporal mechanisms into a cortical framework for sequence processing. In *Neural, Symbolic and Reinforcement methods for sequence learning*, Lecture Notes in Computer Science. Springer, 2001.

[16] F. Gaspard and T. Viéville. Non linear minimization and visual localization of a plane. In *The 6th International Conference on Information Systems, Analysis and Synthesis*, volume VIII, pages 366–371, 2000.

[17] P. Gaussier, A. Revel, J. Banquet, and V. Babeau. From view cells and place cells to cognitive map learning : the hippocampus as a spatio-temporal memory. *Biological Cybernetics*, 86(1), 2002.

[18] I. Howard. *Human Visual Orientation*. John Wiley and Sons, New-York, 1985.

[19] J.-C. Latombe. *Robot motion planning*, volume 124 of *Kluwer international series in engineering and computer science*. Kluwer, 1991.

[20] J. O'Keefe. Do hippocampal pyramidal cells signal non-spatial as well as spatial information. *Hippocampus*, 9:352–364, 1999.

[21] J. O'Keefe and J. Dostrovsky. The hippocampus as a spatial map: preliminary evidence from unit activity in the freely moving rat. *Brain Res.*, 34:171–175, 1971.

[22] J. O'Keefe and L. Nadel. *The hippocampus as a cognitive map*. Oxford Uni. Press, 1978.

[23] J. Petitot and Y. Tondut. Vers une neuro-géométrie. fibrations corticales, structures de contact et contours subjectifs modaux. *Mathématiques, Informatique et Sciences Humaines*, 145:5–101, 1999.

[24] D. Philipona, J. O. Regan, and J.-P. Nadal. Is there something out there? inferring space from sensorimotor dependencies. *Neural Computation*, 15(9), 2003.

[25] B. Poucet, P.-P. Lenck-Santini, V. Hok, E. Save, J.-P. Banquet, and P. Gaussier. Spatial navigation and hippocampal place cell firing: The problem of goal encoding. *Reviews in the Neurosciences*, 15:89–107, 2004.

[26] A. D. Redish. *Contributions to a Computational Neuroscience Theory of Rodent Navigation*. PhD thesis, Carnegie Mellon Univ., Pittsburgh, 1997.

[27] A. Samsonovich and B. McNaughton. Path integration and cognitive mapping in a continuous attractor neural network model. *Journal of Neuroscience*, 17(15):5900–5920, 1997.

[28] W. Skaggs, J. Knierim, H. Kudrimoti, and B. McNaughton. A model of the neural basis of the rat's sense of direction. *Adv. Neural Inf. Process Syst.*, 7:173–80, 1995.

[29] E. Tolman. Cognitive maps in rats and men. *Psychological review*, 5:189–208, 1948.

[30] S. Trullier, S. I. Wiener, A. Berthoz, and J. A. Meyer. Biologically based artificial navigation systems: review and prospects. *Progress in Neurobiology*, 51:483–544, 1997.

[31] T. Viéville. An abstract view of biological neural networks. Technical Report RR-5657, INRIA, Aug. 2005.

[32] T. Viéville. An improved biologically plausible trajectory generator. Technical report, INRIA, Feb. 2006. in press.

[33] T. Viéville and S. Crahay. A deterministic biologically plausible classifier. Technical Report 4489, INRIA, June 2002.

[34] T. Viéville, D. Lingrand, and F. Gaspard. Implementing a multi-model estimation method. *The International Journal of Computer Vision*, 44(1), 2001.

[35] T. Viéville and P. Sander. Using pseudo Kalman-filters in the presence of constraints. Technical Report 1669, INRIA, Sophia, France, 1992.

[36] T. Viéville and C. Vadot. Biologically plausible trajectory generators. Technical Report 4539, INRIA, Sept. 2002.

A Using an harmonic potential with unbounded values

We consider a potential $V : \mathcal{U} \rightarrow \mathcal{R}$ at least twice differentiable and so that :

$$\left\{ \begin{array}{rcl} \lim_{\mathbf{x} \rightarrow \partial \mathcal{U}} V(\mathbf{x}) & = & v(\mathbf{x}) \\ \forall \mathbf{x} \in \mathcal{U}, \Delta V(\mathbf{x}) & = & 0 \end{array} \right.$$

with $\mathcal{U}$ compact. This is called a Dirichlet problem. Here $\Delta V(\mathbf{x})$ is the potential Laplacian:

$$\Delta V(\mathbf{x}) = \sum_{i=1..n} \frac{\partial^2 V}{\partial (x^i)^2}(\mathbf{x}) \tag{13}$$

which vanishes in $\mathcal{U}$.

The key point with respect to a standard analysis about such function (see for instance [13] Chap2.2) is that here, $v(\mathbf{x})$ defined on $\partial \mathcal{U}$, has its values in $\bar{\mathcal{R}} = \mathcal{R} \cup \{-\infty, +\infty\}$.

Let us thus revisit this small part of the partial differential equations theory, discussing our specific case:

$\mathcal{P}_0$ **The fundamental radial symmetric solution.** Let us define, for $n > 2$ (the case $n = 2$ is going to be discussed in the sequel) and a suitable constant σ_n, the function, well-defined for all $\mathbf{x} \neq 0$:

$$\Phi(\mathbf{x}) = \frac{1}{\sigma_n} \left\{ \begin{array}{ll} \frac{1}{(n-2)\,||\mathbf{x}||^{n-2}} & n > 2 \\ -\log(||\mathbf{x}||) & n = 2 \end{array} \right. \tag{14}$$

with $\nabla \Phi(\mathbf{x}) = -\frac{1}{\sigma_n} \frac{\mathbf{x}}{||\mathbf{x}||^n}$ and such that $\mathbf{x} \neq 0 \Rightarrow \Delta \Phi(\mathbf{x}) = 0$.

More precisely $\Delta \Phi(\mathbf{x}) = -\delta(\mathbf{x})$ with $\sigma_n = \frac{n\,\Pi^{n/2}}{\Gamma(n/2+1)}$ (the surface of the boundary of a ball of radius 1 in $\mathcal{R}^n$), $\delta()$ being the Dirac distribution.

This function is the fundamental solution of the equation $\Delta V = 0$ with a radial symmetry (i.e. which depends only on $\mathbf{x}$ magnitude but not on its orientation) and without any boundary condition. Any function of this kind is of the form $a + b\,\Phi(\mathbf{x})$ [13].

$\mathcal{P}_1$ **Mean value property.** An harmonic potential is characterized by the following mean value property:

$$\begin{array}{c} \forall \mathbf{x} \in \mathcal{U}, \forall \rho \in \mathcal{R}+,\ V(\mathbf{x}) = \int_{\partial B(\mathbf{x},\rho)} V(\mathbf{y})\, dS_{\mathbf{y}} \Big/ \int_{\partial B(\mathbf{x},\rho)} dS_{\mathbf{y}} \\ \Leftrightarrow \\ \forall \mathbf{x} \in \mathcal{U},\ \Delta V(\mathbf{x}) = 0 \end{array}$$

where $\partial B(\mathbf{x}, \rho) = \{\mathbf{y}, ||\mathbf{x} - \mathbf{y}|| = \rho\}$ is the boundary of balls centered on $\mathbf{x}$. We also have:

$$V(\mathbf{x}) = \int_{B(\mathbf{x},\rho)} V(\mathbf{y})\, d\mathbf{y} \Big/ \int_{B(\mathbf{x},\rho)} d\mathbf{y} \text{ with } B(\mathbf{x}, \rho) = \{\mathbf{y}, ||\mathbf{x} - \mathbf{y}|| < \rho\}$$

This property is shown, from the 1st Green formula, by a local derivation inside $\mathcal{U}$. It is thus fully valid in our specific case.

$\mathcal{P}_2$ **Maximum principle.** An harmonic potential which is not constant has extremal (minimum / maximum) values only on the boundaries $\partial\mathcal{U}$ of the domain.

As a special case, an harmonic function:

- equal to zero on $\partial\mathcal{U}$ in equal to zero in $\mathcal{U}$,
- defined on a unbounded domain must have infinite values at infinity.

This property is based on the following consequence of the mean value property: if there exists a point $\mathbf{x}$ in $\mathcal{U}$ where the potential is maximum, it is thus constant in the whole connected component of this point. *Here again, this result does not make any use of boundary values. Its consequence is thus also still valid in our case.*

$\mathcal{P}_3$ **Existence, unicity and differentiability.** Such a solution exists. It is unique if and only if $v(\mathbf{x})$ is <u>bounded</u>.

Such a function is differentiable at any order (more generally analytic) *in* $\mathcal{U}$ (but is not necessarily differentiable or even continuous on the border $\partial\mathcal{U}$).

Its derivatives are also harmonic.

In our case we can partially re-use the standard results with the following trick:
- we consider as boundary condition $v_M(\mathbf{x}) = \pm M$ *with* $0 < M < +\infty$ *instead of infinite values* $\pm\infty$*,*
- we apply standard results to this modified problem,
- we finally consider the limit of the results when $M \to +\infty$*. This is valid because of the following:*

> [$\mathcal{P}_4$ **limit property.**] A series of continuous harmonic function which uniformly converges on $\partial\mathcal{U}$, also converge in $\mathcal{U}$ towards an harmonic function.

We thus can conclude about the existence and differentiability of the solution.

There is however not unicity of the solution, because if our trick converges to a solution, another trick may converge to another solution, etc... This is the case for the adelician which represents an infinite family of solutions.

Note that, here, $v(\mathbf{x})$ *is not unconstrained but must be the uniform limit of a bounded potential, which is easily the case in our construction using usual uniform series to obtain* $M \to +\infty$*.*

$\mathcal{P}_5$ **Dirichlet principle.** The solution, if $v(\mathbf{x})$ is <u>bounded</u>, is given by the following optimization problem:

$$V = \arg\min_u max_\lambda \int_{\mathcal{U}} ||\nabla u||^2 + \int_{\partial\mathcal{U}} \lambda^T (u - v)$$

where λ is a Lagrangian multiplicator function which allows to verify the constraints at the domain border.

For an harmonic function, the mean value of the square of the gradient magnitude is thus minimal.

Although easy to derive using the same trick of a bounded boundary condition with a "very high" value, this result does not hold as it because the underlying technics of optimization with constraints (i.e. the saddle point principle) require bounded values.

Regarding the mean gradient squared magnitude property, let us consider any domain $\mathcal{V} \subset\subset \mathcal{U}$. In $\mathcal{U}$, the adelician remains bounded and the Dirichlet principle holds. It is thus verified inside $\mathcal{U}$ as mentioned in this paper.

$\mathcal{P}_6$ **The Green formula.** The solution, if $v(\mathbf{x})$ is integrable, is formally represented (writing $\frac{\partial u}{\partial \nu} = \nabla u \cdot \nu$ the derivate of a function u along the *normal* ν on the domain border $\partial\mathcal{U}$) by the Green formula. Let us rewrite it in two forms:

$$\begin{array}{rcl} V(\mathbf{x}) & = & \int_{\partial\mathcal{U}} \Phi(\mathbf{y}-\mathbf{x}) \frac{\partial V}{\partial \nu}(\mathbf{y})\, d\mathbf{y} - \int_{\partial\mathcal{U}} v(\mathbf{y}) \frac{\partial \Phi}{\partial \nu}(\mathbf{y}-\mathbf{x})\, d\mathbf{y} \\ & = & -\int_{\partial\mathcal{U}} v(\mathbf{y}) \frac{\partial G}{\partial \nu}(\mathbf{x},\mathbf{y})\, d\mathbf{y} \end{array}$$

The Green function: $G(\mathbf{x},\mathbf{y}) = \Phi(\mathbf{y}-\mathbf{x}) - \phi_{\mathbf{x}}(\mathbf{y})$ defined from (14) for $\mathbf{x},\mathbf{y} \in \mathcal{U}, \mathbf{x} \neq \mathbf{y}$, which is symmetric in $\mathbf{x}$ and $\mathbf{y}$, is based on the computation of a "corrector" $\phi_{\mathbf{x}}(\mathbf{y})$ solution of the equations:

$$\left\{ \begin{array}{rcll} \phi_{\mathbf{x}}(\mathbf{y}) & = & \Phi(\mathbf{y}-\mathbf{x}) & \mathbf{y} \in \partial\mathcal{U} \\ \Delta\phi_{\mathbf{x}}(\mathbf{y}) & = & 0 & \mathbf{y} \in \mathcal{U} \end{array} \right.$$

In fact, the calculation of $\phi_{\mathbf{x}}$ is intractable in practice as soon as $\mathcal{U}$ is somehow general.

This result is not easily generalizable in our case, although true as soon as $v(\mathbf{x})$ is integrable because $\frac{\partial G}{\partial \nu}$ is bounded while the previous integral is defined if and only if $v(\mathbf{x})$ is also integrable. This allows $v(\mathbf{x})$ to take unbounded values but only in a sparse sub-set with a null measure. Our problem does not correspond to this specific case.

A step ahead, note that the adelician is built as the Green formula, from integrals defined on the domain border. In the general case, the Green formula is not usable because the related expressions are intractable. This is not the case here.

As a conclusion, an adelician is *not* a standard solution to a Dirichlet problem, some properties not being generalizable "as it" to this limit case. It is still a usable framework, to be used with caution, as detailed here.

Unité de recherche INRIA Sophia Antipolis
2004, route des Lucioles - BP 93 - 06902 Sophia Antipolis Cedex (France)

Unité de recherche INRIA Futurs : Parc Club Orsay Université - ZAC des Vignes
4, rue Jacques Monod - 91893 ORSAY Cedex (France)
Unité de recherche INRIA Lorraine : LORIA, Technopôle de Nancy-Brabois - Campus scientifique
615, rue du Jardin Botanique - BP 101 - 54602 Villers-lès-Nancy Cedex (France)
Unité de recherche INRIA Rennes : IRISA, Campus universitaire de Beaulieu - 35042 Rennes Cedex (France)
Unité de recherche INRIA Rhône-Alpes : 655, avenue de l'Europe - 38334 Montbonnot Saint-Ismier (France)
Unité de recherche INRIA Rocquencourt : Domaine de Voluceau - Rocquencourt - BP 105 - 78153 Le Chesnay Cedex (France)

Éditeur
INRIA - Domaine de Voluceau - Rocquencourt, BP 105 - 78153 Le Chesnay Cedex (France)
http://www.inria.fr
ISSN 0249-6399